

## CALIBRATION OF MODELS WITH MICROSHADE

Søren Østergaard Jensen

Soren.O.Jensen@teknologisk.dk

Danish Technological Institut, Energy and Climate Division  
Gregersensvej, DK-2630 Taastrup, Denmark

### ABSTRACT

This paper deals with the calibration of models capable of simulating the performance of MicroShade™. The function of MicroShade is similar to Venetian blinds, however, MicroShade is a microstructure embedded in a metal foil with a thickness of less than one mm. MicroShade has been modelled using a novel module in ESP-r for modelling bidirectional transmission through transparent multilayered constructions. Windows with and without MicroShade have been tested in two dedicated test rooms. The measurements from the test rooms have been used to calibrate the model of MicroShade. Finally simulations are used to show how MicroShade will perform in a real building.

### INTRODUCTION

MicroShade™ is a microstructure of small holes. Figure 1 shows an example of MicroShade. MicroShade consists of many small super elliptic shaped holes manufactured in a thin stainless steel sheet – see figure 1. The holes have a tilting angle and resemble the way Venetian Blinds function. However, the appearance is different and so is the view out as seen in figure 3. Newer versions of MicroShade have twice the distance between the opaque stripes shown in figure 3. The screening off and view out through MicroShade are determined by the shape and tilting angle of the holes in figure 1.

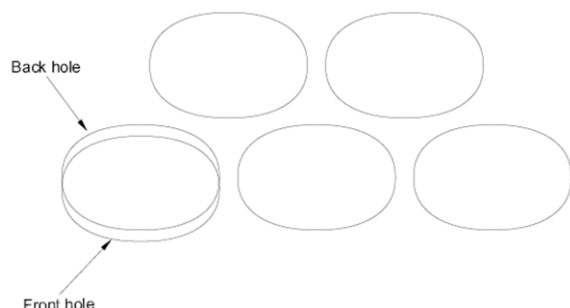


Figure 1 Example of the holes in MicroShade. The width of the holes are less than 1 mm.

Figure 24 shows MicroShade imbedded in a low-e window. The name of this product is MicroShade™ IG (Insulated Glazing) but will in the following be referred to as MicroShade windows.

The model of MicroShade is a matrix where the total direct transmission, the absorption in each layer of the window and the enhancement of incoming diffuse radiation due to the scattering of direct radiation in the MicroShade are listed for combinations of the horizontal and vertical incidence angle at steps of 5°. The values of the matrix are generated by a special purpose program where the main parameter is the projected hole area seen by the sun at different incidence angles and optical properties of MicroShade and glass. An example of the matrix is included at the end of the paper.



Figure 2 The view out of a traditional low-e window with solar control coating in test room B. g-value of the window: 0.37.



Figure 3 The view out of test room A with a low-e window with MicroShade.

Figure 4 shows the function of MicroShade. Figure 4 shows the transmittance of direct solar radiation through the two windows in figures 2 and 3 at an azimuth of 0°. During winter at low solar heights when solar heat is valuable the two windows let in almost the same amount of solar heat. But during summer at high solar heights and risk of overheating the MicroShade lets in considerably less solar heat than the traditional window with solar control coating.

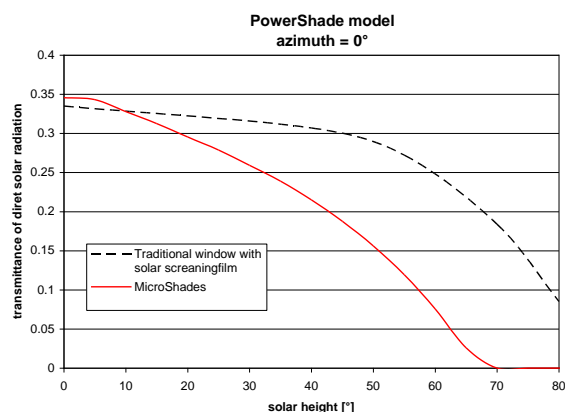


Figure 4 The transmittance of direct solar radiation through the two windows in figures 2 and 3 at an azimuth of 0°.

A special type of MicroShade is PowerShade. These are similar to MicroShade but are coated with solar cells on the surface facing the outside. PowerShades are currently under development. More information on PowerShade/MicroShade can be found on [www.photosolar.dk](http://www.photosolar.dk).

## TEST ROOMS

MicroShade and traditional windows were tested side-by-side in two well-defined and heavily monitored test rooms at Danish Technological Institute, Taastrup, Denmark. The floor area and volume of the test rooms were 6.84 m<sup>2</sup> and 16.73 m<sup>3</sup> respectively. The window of each test room consisted of two transparent areas of totalling 1.98 m<sup>2</sup>.

The test rooms, the thermo-physical properties of the materials of the test rooms and the monitoring system are described in detail in (Jensen, 2008a).

## CALIBRATION OF THE MODELS

A model of the two test rooms was developed in the simulation program ESP-r (ESRU, 2001).

A step by step approach was applied in the calibration of the ESP-r and MicroShade models:

- Step 1. Calibration of the solar radiation on the facade
- Step 2. Calibration of the model of the traditional window
- Step 3. Calibration of the diffuse radiation through the MicroShade window
- Step 4. Calibration of the MicroShade model

Step 5. Calibration of the thermal model of the test rooms. However, this step will not be dealt with in this paper

The above calibration steps are documented in details in (Jensen, 2008b).

For the calibration exercises measurements from three periods in 2008 were chosen:

Table 1

The three measuring periods applied in the calibration exercise.

Season	Period	Solar height °
Winter	21/1-17/2 2008	14.4-22.7
Spring (autumn)	25/3-26/4 2008	36.1-47.8
Summer	1-28/6 2008	56.5-57.8

## Calibration of the solar radiation on the facade

The input to the simulation program was the global solar radiation and the horizontal diffuse radiation on the roof just above the test rooms using calibrated precision pyranometers. The solar measuring station is shown in figure 5. The solar radiation on the façade was also measured with a calibrated precision pyranometer.



Figure 5 The solar measuring station.

Figure 6 shows an example of the comparison between measured and calculated solar radiation on the façade. The other periods show similar agreement (Jensen, 2008b). In order to obtain this very good agreement it was necessary to use an albedo of only 0.05. This is a low value but may be justified when considering that the façade faces a courtyard where the surfaces of the surrounding buildings are in the shade most of the time.

The standard solar algorithms in ESP-r for calculation of solar radiation were applied in the calibration

## Calibration of the model of the traditional window

Calibrated precision pyranometers were applied for measuring the solar radiation entering the rooms.

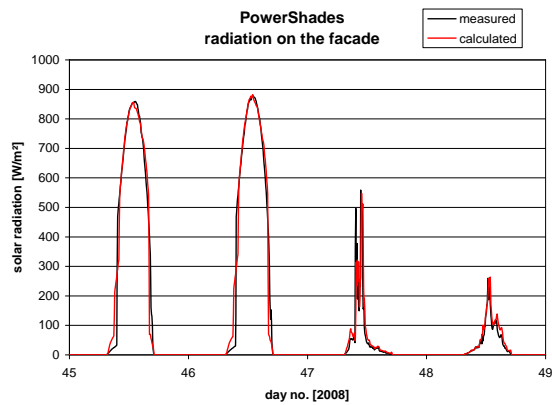


Figure 6 Comparison between measured and calculated solar radiation on the facade

Although the project concerned MicroShade the model of the traditional window was also calibrated. The reason for this was that both windows are low-e windows with at low-e coating. This coating changes the spectral distribution of solar radiation which might influence the accuracy of the pyranometers. However, the transmittance through a traditional window is very well-defined. So if good agreement is obtained between measured and calculated solar radiation for the traditional window it is implied that the pyranometers are capable of measuring the solar radiation coming through the MicroShade window. In fact such a calibration exercise is also a validation exercise on the pyranometers behind the windows.

Figure 7 shows a comparison between measured and calculated incoming solar radiation through the traditional window. The other periods show similar agreement (Jensen, 2008b).

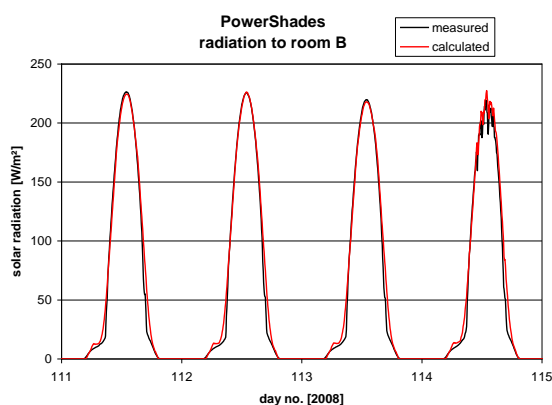


Figure 7 Comparison between measured and calculated solar radiation through the traditional window.

Based on the above it was concluded that the model of the traditional window was precise enough and that the measured solar radiation through the MicroShade window was applicable for calibration of the model of the MicroShade window.

## Calibration of the diffuse radiation through the MicroShade

The matrix shown at the end of the paper is automatically generated by a special purpose program where the input is the geometry of the holes shown in figure 1. The program calculates for combinations of all vertical and horizontal incidence angles of the sun the total transmittance of direct radiation, the absorption in each layer of the window and the enhancement of the transmitted diffuse radiation due to scattering of direct radiation in the MicroShade. However, so far no model or experience exists on how to calculate the transmittance of diffuse radiation through MicroShades. Therefore, the transmittance of diffuse radiation is here found empirically by using the measured data from the test rooms. Days with only diffuse radiation have been chosen. During those days the ratio between the solar radiation on the façade and through the MicroShade window was calculated as shown in figure 8. That ratio is the transmittance of diffuse radiation.

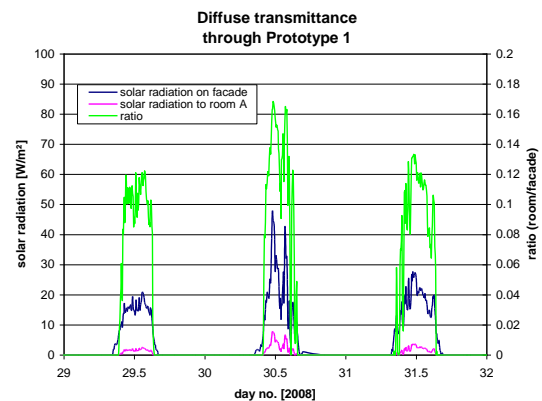


Figure 8 The solar radiation on the façade and to room A together with the ratio (= transmittance of diffuse radiation) for three days in January 2008 with overcast conditions.

Unfortunately, there were only few days with overcast conditions during the first half of 2008 – and that is not normal for Danish weather conditions. Figure 9 shows the calculated transmittance for those few days. The values in figure 9 should be similar or even higher during the winter due to the lower solar height but an opposite tendency is seen – increasing transmittance with increasing solar height. The increasing tendency is assumed to be caused by two facts:

1. solar radiation during January (two first points in figure 9) was very low and therefore the uncertainty is very high.
2. there might have been some direct radiation at high solar heights (two-three last points in figure 9).

Figure 9 shows that there is a need for the development of a rigid calculation method for the diffuse radiation through MicroShade. Such method are being developed when writing this. However, for the

calibration study a diffuse transmittance coefficient of 0.12 was chosen.

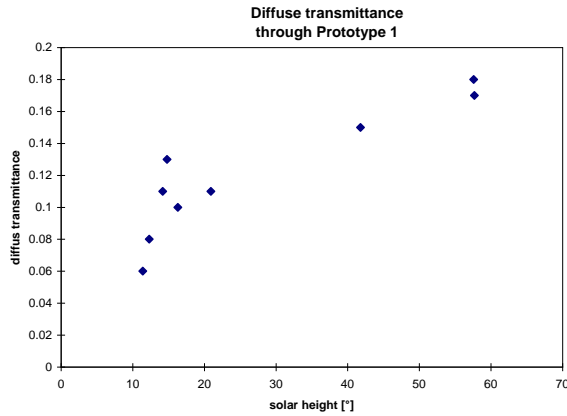


Figure 9 The transmittance of diffuse radiation dependent on solar height.

### Calibration of the MicroShade model

A novel module for modelling bidirectional transmission through transparent multilayered constructions (developed in the project (Teknologisk Institute, 2005)) has been used in the following exercises. As input the module uses the matrix shown in figure 24. Using the special purpose program mentioned on the previous page the matrix for the actual MicroShade was generated and applied in the model of the test rooms. Figure 10 shows a comparison between measured and calculated solar radiation through the MicroShade window.

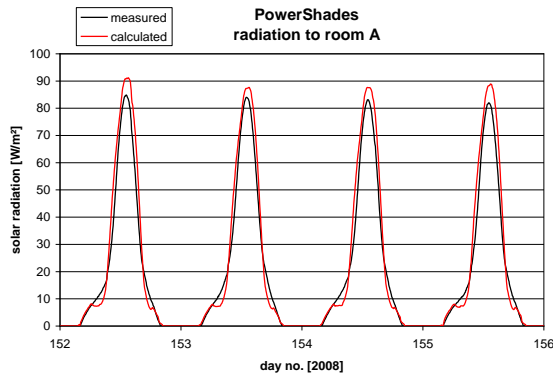


Figure 10 Measured and calculated solar radiation through the MicroShade window.

Figure 10 shows that the model overestimates the incoming solar radiation at noon and underestimates the incoming solar radiation at early morning and late afternoon. The main problem is the overestimation at noon as there is only a small amount of energy in the solar radiation at early morning and late afternoon.

As a first attempt the transmittance of direct solar radiation in the matrix was simply multiplied by an empirically found factor (using measurements from

all three measuring periods) dependent on the solar height:

$$fs = -0.002 \cdot sh + 1.0529 \quad (1)$$

where: sh is the solar height

Figure 11 shows the result of applying this factor in the calculations.

The agreement is now much better but still not good enough as shown in figure 12. This close-up reveals that an overestimation also occurs before and after noon. Figure 13 shows the relative overestimation during six days in July 2006.

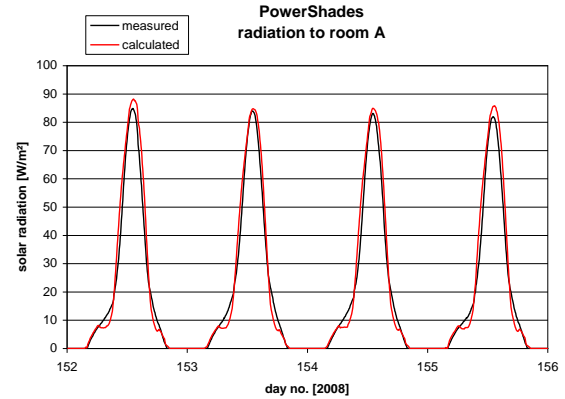


Figure 11 Measured and calculated solar radiation through the MicroShade window using the modified model - based on solar height.

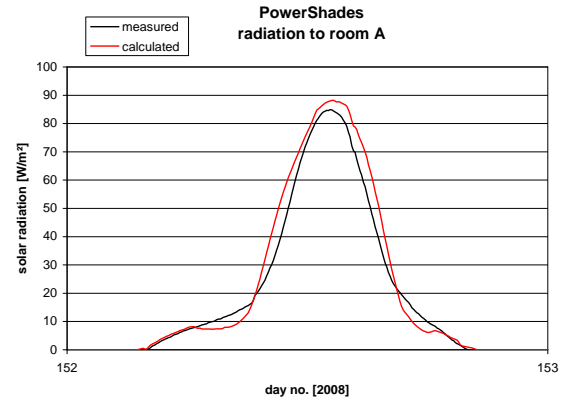


Figure 12 Close-up of figure 11.

Based on figure 13 a new correction factor dependent on the relative azimuth (azimuth relative to the facade) was developed:

$$fa = -3.6223 \cdot 10^{-12} \cdot x^6 - 4.9168 \cdot 10^{-11} \cdot x^5 + 5.343 \cdot 10^{-8} \cdot x^4 + 5 \cdot 10^{-7} \cdot x^3 - .982 \cdot 10^{-4} \cdot x^2 - 9.108 \cdot 10^{-4} \cdot x + 1.0338 \quad (2)$$

for  $fa < 1$ , for  $fa \geq 1$   $fa$  is set to 1

where: x is the relative azimuth. The relative azimuth is zero when the sun vertically is perpendicular to the facade.

Figures 14-15 shows the result of applying this factor in the calculations.

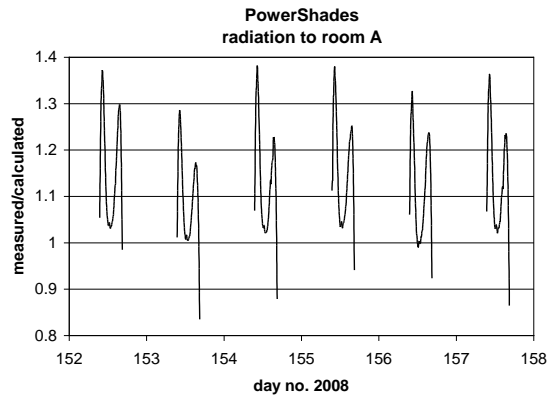


Figure 13 The relative overestimation.

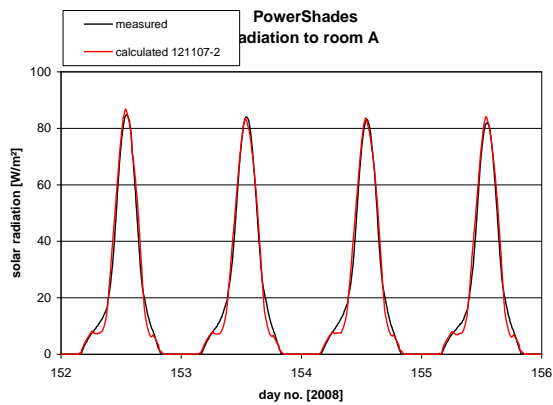


Figure 14 Measured and calculated solar radiation through the MicroShade window using the modified model called 121107-2 - based on solar height and relative azimuth.

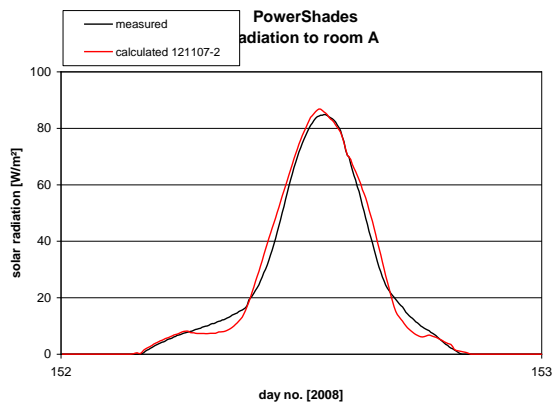


Figure 15 Clos-up of figure 14.

Figures 14 and 15 shows very good agreement between measured and calculated solar radiation through the MicroShade window.

The other periods show similar agreement (Jensen, 2008b) – both for clear sky and overcast conditions – as shown in the following figures. However, there was some underestimation during clear sky conditions at low solar heights as shown in figure 19.

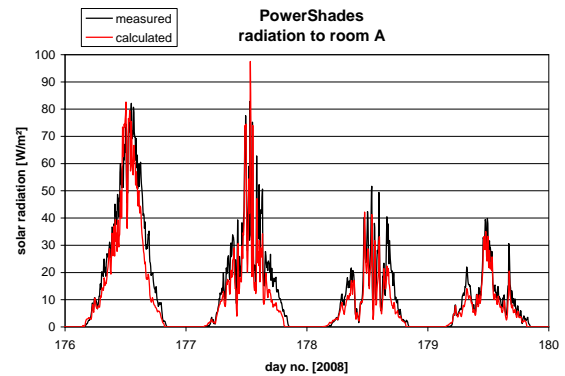


Figure 16 Measured and calculated solar radiation through the MicroShade window using the modified model 121107-2.

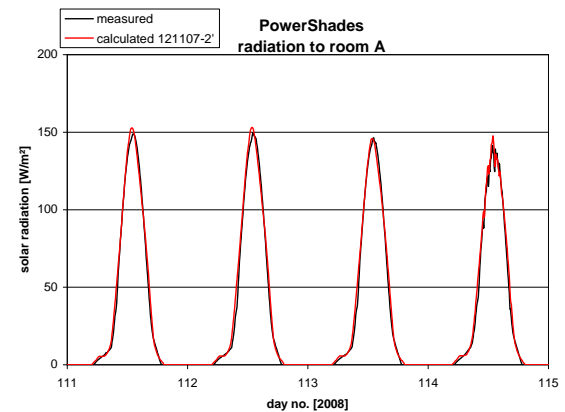


Figure 17 Measured and calculated solar radiation through the MicroShade window using the modified model 121107-2.

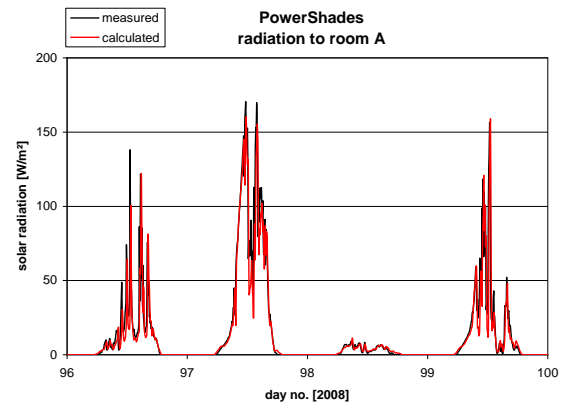


Figure 18 Measured and calculated solar radiation through the MicroShade window using the modified model 121107-2.

The above calibration exercise is to show that it is possible to generate a matrix/model of MicroShade windows, which represents the optical properties of MicroShade windows very well. The findings from the above calibration exercise will be utilized to modify the special purpose program that generates



the matrix so measurements no longer will be necessary in order to establish a well-matching matrix. The new version of the program will to more precisely describe the transmission of both direct and diffuse solar radiation through windows with MicroShades. The new program will be tested in a new validation exercise. A reliable program will ease the development of Micro- and PowerShade considerably as it is cheaper to perform parametric studies using a computer model than to perform measurements.

Figure 20 shows that the intention from figure 4 regarding MicroShade has been fulfilled. Figure 20 shows based on measurements that the investigated MicroShade during the summer at noon decreases the amount of incoming solar radiation with 50% compared to a traditional window with solar control coating, while letting the same amount of solar radiation in during the winter where solar heating most often is valuable

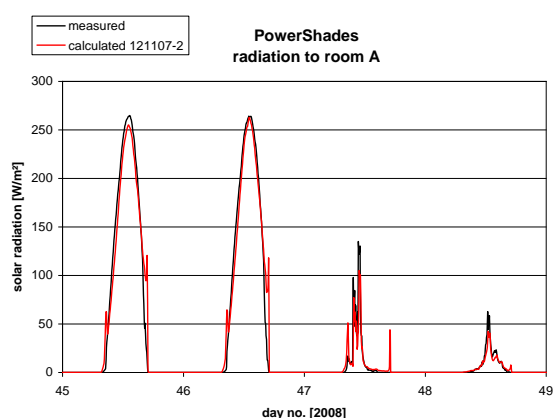


Figure 19 Measured and calculated solar radiation through the MicroShade window using the modified model 121107-2.

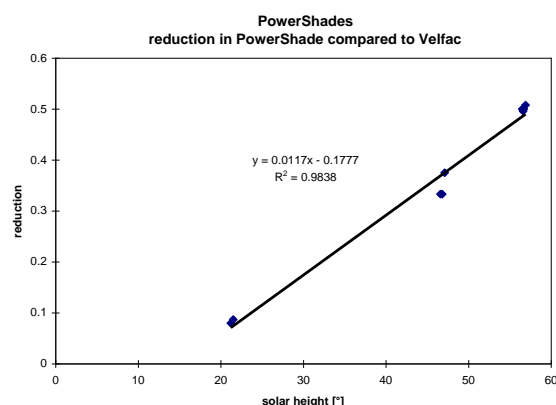


Figure 20 The measured reduction of the transmission of solar radiation due to MicroShade at noon compared to a traditional window with solar control coating.

### Calibration of the thermal model of the test rooms

Although the test rooms are very simple the modelling of them is rather complex and the calibration of

this part of the model is difficult to perform due to the many parameters and large uncertainties. The calibration of the model of the test rooms will not be dealt with here, as the main purpose of the paper is to describe the calibration of the bidirectional model in ESP-r of MicroShade. Please refer to (Jensen, 2008b) if interested in step 5 of the calibration procedure.

Here it will only be stated that the investigated MicroShade (in the test room) is capable of lowering the peak temperature in the test room at noon with up to 2 K compared to the traditional window with solar control coating. MicroShade may thus reduce potential overheating risks and decrease the cooling demand. This is shown in the following paragraph.

### THE PERFORMANCE OF MICRO-SHADES IN REAL BUILDINGS

It has been shown that although not perfect the model 121107-2 represent the optical performance of a MicroShade window rather well. Using this model it will in the following be shown how this type of solar control device performs compared to other solar shading measures.

ESP-r has been used to simulate the performance of MicroShade in a real Danish building. The building was designed by the world famous architects “Henning Larsen”. The building is the domicile of a bank and it is situated in the centre of Copenhagen. Figure 21 shows the north façade of the building. The figure shows the transparency of the building.

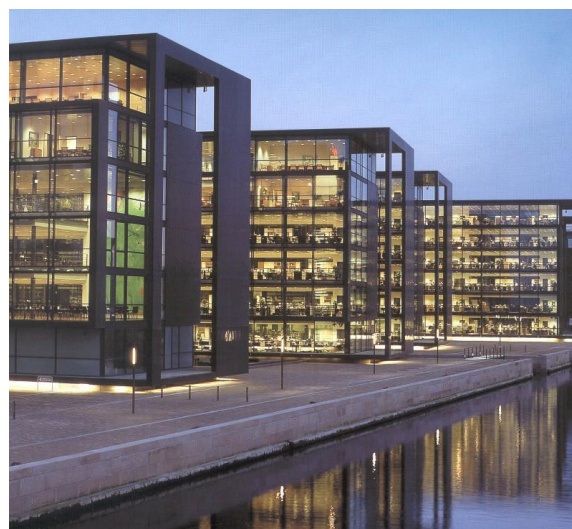


Figure 21 The north facing facades of the building.

90% of the south and north facades are transparent so extensive solar control is necessary in order to reduce the overheating problems and thereby reduce the cooling load and energy demand of the building. The glazing of the facades has solar control coating which reduces the g-value of the windows to 0.32 – i.e. rather similar to the original traditional window dealt with earlier in this paper. This very low g-value is, however, not sufficient for ensuring a comfortable indoor climate in the building so external solar shad-

ing has been added to the south facades as seen in figure 22.



Figure 22 One south façade of the building.

As shown in figure 23 the external solar shading consists of movable lamellas made of glass with silk screen printing. The lamellas follow automatically the position of the sun (the solar height) over the day - ie the lamellas are always perpendicular to the beam radiation so that all direct solar radiation hits the lamellas before hitting the windows.



Figure 23 The external solar shading consisting of glass lamellas with silk screen printing.

Due to the silk screen printing on glass there is still some outlook through the window even when the lamellas are closed.

The combination of solar control glass and external solar shading gives an overall g-value of app. 0.17 – which is very low.

An ESP-r model of the building was developed in an earlier project (Danish Technological Institute, 2005) – please refer to this for further information. The U-value for the facades are  $1.12 \text{ W/m}^2$ . The ventilation system maintain an air change rate of  $5^{\text{h}}$ . The internal heat gain is during office hours  $49 \text{ W/m}^2$ .

In the present case, only one floor of the building has been simulated. The floor area is  $642 \text{ m}^2$ .

Simulations have been carried out with four different types of south facades:

- the present south façade with at g-value of 0.17 – figure 23
- the present south façade without the external solar shading device
- MicroShade using the calibrated model 121107-2
- MicroShade using the non-calibrated model applied in figure 10 (called model 121107). The reason for this is to show the necessity of calibration of the MicroShade model.

Table 2 Absolute annual cooling demand and relative demand compared to the present situation. The column in % after the cooling demand in kWh states how much larger (in %) the cooling demand is compared to the present situation.

Facade	Cooling demand	
	kWh	%
Present, g-value: 0.17	6106	-
Present without external solar shade, g-value: 0.32	9091	49
MicroShade, 121107	7483	23
MicroShade, 121107-2	6584	8

121107-2 performs almost as well as the present rather complex solar control system and much better than traditional sun control glass.

In addition table 2 shows the importance of a correct model of the solar transmittance through the MicroShade. The cooling demand with 121107 is app. 15 % higher than with 121107-2.

The simulations also show that there is hardly any difference in the heating load between the four systems in table 2. The difference in electricity demand for artificial lightning should also be compared but is beyond the scope of the work behind this paper.

## CONCLUSION

The described work shows that via calibration using measured data from test rooms it is possible to obtain a model that represents the complex optical performance of MicroShade very well. The model of MicroShade has been developed using the bidirectional transmission module for transparent multilayered constructions in the simulation program ESP-r.

The purpose of MicroShade is to reduce the overheating risk during the summer with large solar heights. The measurements show that the objective of MicroShade was met as the incoming solar energy was reduced by about 50% in the summer at noon compared to a traditional window with solar control coating and a g-value of 0.37.

Simulations on a real building show that the cooling demand in this particular building is in the same order of magnitude when using Micro-Shades as when considering the existing rather complex external solar shading system together with windows with solar control coating (g-value: 0.17).

## ACKNOWLEDGEMENT

The work presented in this paper has been financed by Energinet.dk.

The described work was performed in cooperation with the Danish firm PhotoSolar that develops/produces MicroShade™ and PowerShade.

## REFERENCES

ESRU, 2001. Data Model Summary – ESP-r – Version 9 series. Energy Systems Research Unit, University of Strathclyde. December 2001.

Jensen, S.Ø., 2008a. Test rooms for test of PowerShades. Danish Technological Institute. ISBN 87-7756-769-2

Jensen, S.Ø., 2008b. Test of PowerShades and calibration of models with PowerShades. Danish Technological Institute. ISBN 87-7756-770-6.

Technological Institute, 2005. Transparent solar cells – the electricity producing solar shading of the future (in Danish). PEC Group, Danish Technological Institute.

\*BIDIRECTIONAL

\*types,1

\*item,121107

\*layers,5,glass1,shading,glass2,air,glass3

\*sets,1 # there is only this set of optical data

\*start\_set

\*diffuse\_abs,0.036,0.372,0.013,0.000,0.042

\*diffuse\_trn,0.12

\*direct\_angs,37,37

\*data

#Incidence angle, Total Glass 1, Shading device, Glass 2, Air, Glass 3, Converted diffuse fraction

#HorizontVertical, Transmittance, Absorb, Absorb, Absorb, Absorb, Absorb, Direct-diffuse

#Degrees, Degrees

-90 -90 0 0 0 0 0 0

-90 -85 0 0 0 0 0 0

-90 -80 0 0 0 0 0 0

-90 -75 0 0 0 0 0 0

-90 -70 0 0 0 0 0 0

-90 -65 0 0 0 0 0 0

-90 -60 0 0 0 0 0 0

-90 -55 0 0 0 0 0 0

-90 -50 0 0 0 0 0 0

-90 -45 0 0 0 0 0 0

-90 -40 0 0 0 0 0 0

-90 -35 0 0 0 0 0 0

-90 -30 0 0 0 0 0 0

-90 -25 0 0 0 0 0 0

-90 -20 0 0 0 0 0 0

-90 -15 0 0 0 0 0 0

-90 -10 0 0 0 0 0 0

-90 -5 0 0 0 0 0 0

-90 0 0 0 0 0 0 0

-90 5 0 0 0 0 0 0

-90 10 0 0 0 0 0 0

-90 15 0 0 0 0 0 0

-90 20 0 0 0 0 0 0

-90 25 0 0 0 0 0 0

-90 30 0 0 0 0 0 0

-90 35 0 0 0 0 0 0

-90 40 0 0 0 0 0 0

-90 45 0 0 0 0 0 0

-90 50 0 0 0 0 0 0

-90 55 0 0 0 0 0 0

-90 60 0 0 0 0 0 0

-90 65 0 0 0 0 0 0

-90 70 0 0 0 0 0 0

-90 75 0 0 0 0 0 0

-90 80 0 0 0 0 0 0

-90 85 0 0 0 0 0 0

-90 90 0 0 0 0 0 0

-85 -90 0 0 0 0 0 0

-85 -85 0 0.022 0 0 0 0

-85 -80 0 0.039 0.003 0 0 0

-85 -75 0 0.039 0.02 0 0 0.001

-85 -70 0 0.039 0.035 0 0 0.002

-85 -65 0 0.039 0.05 0 0 0.003

1<sup>th</sup> column: azimuth

2<sup>th</sup> column: solar height

3<sup>th</sup> column: total direct transmittance

4<sup>th</sup> column: absorption in the outer layer of glass

5<sup>th</sup> column: absorption in the PowerShade foil

6<sup>th</sup> column: absorption in the in the glass behind the PowerShade foil

7<sup>th</sup> column: absorption in the air gab of the window

8<sup>th</sup> column: absorption in the inner layer of glass

9<sup>th</sup> column: enhancement of diffuse radiation due to scattering of direct radiation in the PowerShade fail

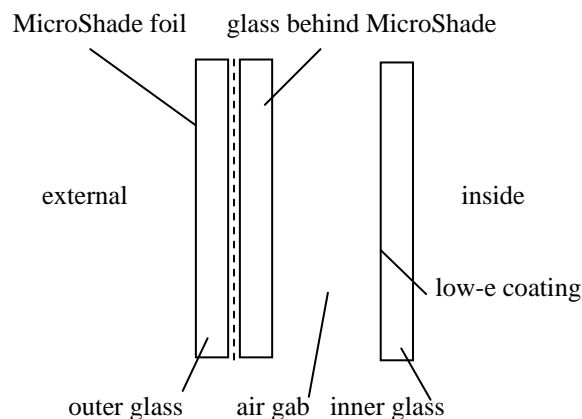


Figure 25 Example of a MicroShade matrix. The matrix covers azimuths and solar heights from -90 to 90° with steps of 5°.